POD-DEIM APPROACH ON DIMENSION REDUCTION OF A MULTI-SPECIES HOST-PARASITOID SYSTEM

G. Dimitriu* Razvan Stefanescu† Ionel M. Navon‡

Abstract

In this study, we implement the DEIM algorithm (Discrete Empirical Interpolation Method), combined with POD (Proper Orthogonal Decomposition) to provide dimension reduction of a model describing the aggregative response of parasitoids to hosts in a coupled multi-species system. The model is defined by five reaction-diffusion-chemotaxis equations. We show DEIM improves the efficiency of the POD approximation and achieves a complexity reduction of the nonlinear terms. Numerical results are presented.

MSC: 35K57, 65M06, 65Y20.

keywords: reduced order modeling, proper orthogonal decomposition, discrete empirical interpolation method.

1 Introduction

Reduced order modeling refers to the development of low-dimensional models that represent the important characteristics of a high-dimensional dy-

*dimitriu.gabriel@gmail.com "Grigore T. Popa" University of Medicine and Pharmacy, Department of Mathematics and Informatics, Iaşi 700115, Romania

†Virginia Polytechnic Institute and State University, Computer Science Department, Blacksburg, VA 24060, USA

‡The Florida State University, Department of Scientific Computing, Tallahassee, FL 32306, USA

namical system. Typically, reduced models are constructed by projecting the high-fidelity model onto a suitably chosen low-dimensional subspace [1]. While for linear models it is possible to produce input-independent high accurate reduced models, in the case of general nonlinear systems, the transfer function approach is not applicable and input-specified semi-empirical methods are usually employed. Most approaches for nonlinear problems construct the reduced bases from a collection of simulations (method of snapshots [19, 20, 21]).

Proper Orthogonal Decomposition (POD) – see [3, 5, 9, 10, 14] and the references therein – is probably the mostly used and most successful model reduction technique, where the basis functions contain information from the solutions of the dynamical system at pre-specified time-instances, so-called snapshots. Due to a possible linear dependence or almost linear dependence, the snapshots themselves are not appropriate as a basis. Instead two methods can be employed, singular value decomposition (SVD) for the matrix of snapshots or eigenvalues decomposition for the correlation matrix [22]. The singular valued decomposition based POD basis construction is more computational efficient since it decomposes the snapshots matrix whose condition number is the square root of the correlation matrix used in the eigenvalue decomposition.

A considerable reduction in complexity is achieved by DEIM [7] – a discrete variation of Empirical Interpolation Method (EIM), proposed by Barrault, Maday, Nguyen and Patera in [4]. According to this method, the evaluation of the approximate nonlinear term does not require a prolongation of the reduced state variables back to the original high dimensional state approximation required to evaluate the nonlinearity in the POD approximation.

In this work, we perform an application of DEIM combined with POD to obtain dimension reduction of a model describing the interactions of the two hosts and two parasitoids in a one-dimensional domain in the presence of a chemotaxis process. The model defined was introduced and analyzed by Pearce et al. in [17, 18] with respect to the stability properties of the steady-states. The behaviour of the parasitoids towards plant infochemicals generated during host feeding are defined as a chemotactic response and the plant infochemicals are viewed as chemoattractants. The model considers a single chemoattractant produced in proportion to the total host density. Both parasitoids play the role of biological control agents against the hosts.

The paper is organized as follows. Section 2 describes the equations of parasitoid model under study. Section 3 describes the POD and DEIM methods along with Galerkin projection. Results of illustrative numerical

experiments are discussed in Section 4 while conclusions are drawn in Section 5.

2 The multi-species host-parasitoid model

We describe here the parameters and the model equations introduced by Pearce et al. in [18]. The reaction kinetics describing the interactions between hosts and parasitoids are coupled with spatial motility and chemotaxis terms giving rise to a system of reaction-diffusion-chemotaxis equations.

In the absence of parasitism, both host species are modelled by logistic, density-dependent growth, with growth rates r_1 and r_2 and carrying capacities K_1 and K_2, respectively. Parasitism by both parasitoids is modelled by an Ivlev functional response. *C. glomerata* parasitises *P. brassicae* at rate α_1 and *P. rapae* at rate α_2. *C. rubecula* parasitises *P. rapae* at rate α_3. The efficiency of parasitoid discovery of hosts is denoted by a_1, a_2 and a_3. Each parasitised host gives rise to e_1, e_2 and e_3 next-generation parasitoids. The parasitoids are subject to mortality rates d_1 (*C. glomerata*) and d_2 (*C. rubecula*).

The motility coefficients D_1, D_2, D_3 and D_4 of the four species are constants and determine the rate at which each species disperses randomly throughout the domain. The chemoattractant K is generated proportionally to the total host density $(N + M)$ at the rate r_3 and decays at the rate d_3. The motility coefficient of the chemoattractant, D_5, is a constant and defines the rate at which the chemoattractant diffuses through the domain. The chemotactic response of both species of parasitoid is modelled as a linear response and the strength of the response depends on the chemotaxis coefficients χ_1 and χ_2. The model is defined by the equations ([18]):

$$
\begin{aligned}
\frac{\partial N}{\partial t} &= \overbrace{D_1\nabla^2 N}^{\text{random motility}} + \overbrace{r_1 N\left(1-\frac{N}{K_1}\right)}^{\text{logistic growth}} - \overbrace{\alpha_1 P(1-e^{-a_1 N})}^{\text{mortality due to parasitism}}\,, \\
\frac{\partial M}{\partial t} &= D_2\nabla^2 M + r_2 M\left(1-\frac{M}{K_2}\right) - \alpha_2 P(1-e^{-a_2 M}) \\
&\quad -\alpha_3 Q(1-e^{-a_3 M})\,, \\
\frac{\partial P}{\partial t} &= D_3\nabla^2 P - \chi_1\nabla\cdot(P\nabla k) + e_1\alpha_1 P(1-e^{-a_1 N}) \\
&\quad +e_2\alpha_2 P(1-e^{-a_2 M}) - d_1 P\,, \\
\frac{\partial Q}{\partial t} &= \underbrace{D_4\nabla^2 Q}_{\text{random motility}} - \underbrace{\chi_2\nabla\cdot(Q\nabla k)}_{\text{parasitoid chemotactic response}}
\end{aligned}
\tag{1}
$$

$$
\begin{aligned}
& + \underbrace{e_3\alpha_3 Q(1-e^{-a_3 M})}_{\text{growth to the parasitism}} - \underbrace{d_2 Q}_{\text{mortality}} \ , \\
\frac{\partial K}{\partial t} &= D_5\nabla^2 K + \underbrace{r_3(N+M)}_{\text{production}} - d_3 K \, ,
\end{aligned}
$$

where N and M are the density of hosts *P. brassicae* and *P. rapae*, respectively, P and Q represent the density of parasitoids *C. glomerata* and *C. rubecula* and K represents the concentration of the chemoattractant produced during feeding by the hosts. $N = N(x,t)$ denotes local population density (organisms per area) at time t and spatial coordinate x (and likewise for M, P, and Q). $k = k(x,t)$ denotes local chemoattractant concentration at time t and spatial coordinate x.

Here we consider the system (2) in a bounded domain Ω with smooth boundary $\partial\Omega$ and homogeneous Dirichlet boundary conditions (which correspond to a hostile external habitat). The initial conditions given by $N(x,0) = N_0(x)$, $M(x,0) = M_0(x)$ $P(x,0) = P_0(x)$,$Q(x,0) = Q_0(x)$ and $K(x,0) = K_0(x)$ will be specified in Section 4.

Using the non-dimensional variables: $t' = r_1 t$, $x' = \frac{x}{L}$, $N' = \frac{N}{K_1}$, $M' = \frac{M}{K_2}$, $P' = \frac{P}{K_1}$, $Q' = \frac{Q}{K_2}$, $K' = \frac{K}{K_0}$, and dropping primes one obtains the nondimensionalised system:

$$
\begin{aligned}
\frac{\partial N}{\partial t} &= D_N\nabla^2 N + N\,(1-N) - s_1 P(1-e^{-\rho_1 N}) \, , \\
\frac{\partial M}{\partial t} &= D_M\nabla^2 M + \gamma_1 M\,(1-M) - s_2 P(1-e^{-\rho_2 M}) \\
&\quad -s_3 Q(1-e^{-\rho_3 M}) \, , \\
\frac{\partial P}{\partial t} &= D_P\nabla^2 P - \chi_P\nabla\cdot(P\nabla k) + c_1 P(1-e^{-\rho_1 N}) \\
&\quad +c_2 P(1-e^{-\rho_2 M}) - \eta_1 P \, , \\
\frac{\partial Q}{\partial t} &= D_Q\nabla^2 Q - \chi_2\nabla\cdot(Q\nabla k) + c_3 Q(1-e^{-\rho_3 M}) - \eta_2 Q \, , \\
\frac{\partial K}{\partial t} &= D_K\nabla^2 K + \gamma_2(N+\gamma_3 M) - \eta_3 K
\end{aligned}
\qquad (2)
$$

where $D_N = \frac{D_1}{r_1 L^2}$, $D_M = \frac{D_2}{r_1 L^2}$, $D_P = \frac{D_3}{r_1 L^2}$, $D_Q = \frac{D_4}{r_1 L^2}$, $D_K = \frac{D_5}{r_1 L^2}$, $\chi_P = \frac{\chi_1 k_0}{r_1 L^2}$, $\chi_Q = \frac{\chi_2 k_0}{r_1 L^2}$, $\rho_1 = \frac{a_1}{K_1}$, $\rho_2 = \frac{a_2}{K_2}$, $\rho_3 = \frac{a_3}{K_2}$, $\gamma_1 = \frac{r_1}{r_2}$, $\gamma_2 = \frac{r_3}{K_1} r_1$, $\gamma_3 = \frac{K_2}{K_1}$, $s_1 = \frac{\alpha_1}{r_1}$, $s_2 = \frac{\alpha_2 K_1}{\alpha_1 K_2}$, $s_3 = \frac{\alpha_3}{r_1}$, $c_1 = \frac{e_1\alpha_1}{r_1}$, $c_2 = \frac{e_2\alpha_2}{r_1}$, $c_3 = \frac{e_3\alpha_3}{r_1}$, $\eta_1 = \frac{d_1}{r_1}$, $\eta_2 = \frac{d_2}{r_1}$ and $\eta_3 = \frac{d_3}{r_1}$.

3 The POD and POD-DEIM reduced order systems

In this section we briefly present some details for constructing the reduced-order system of the full-order system (2) applying Proper Orthogonal Decomposition (POD) and Discrete Empirical Interpolation Method (DEIM).

POD is an efficient method for extracting orthonormal basis elements that contain characteristics of the space of expected solutions which is defined as the span of the snapshots ([9, 10]). In this framework, snapshots are the sampled (numerical) solutions at particular time steps or at particular parameter values. POD gives an optimal set of basis vectors minimizing the mean square error of a reduced basis representation.

Our reduced order modeling description uses a discrete inner product though continuous products may be employed too. Generally, an unsteady model is usually governed by the following semi–discrete dynamical system

$$\frac{d\mathbf{y}(t)}{dt} = \mathbf{F}(\mathbf{y}, t), \quad \mathbf{y}(0) = \mathbf{y}_0 \in I\!R^n, \quad n \in I\!N, \tag{3}$$

n being the number of space points discretizing the domain. From the temporal-spatial flow $\mathbf{y}(t) \in I\!R^n$, we select an ensemble of N_t time instances $\mathbf{y}_1, ..., \mathbf{y}_{N_t} \in I\!R^n$, where $N_t \in I\!N,\ N_t > 0$. If we denote by $\bar{\mathbf{y}} = \frac{1}{N}\sum_{i=1}^{n} \mathbf{y}_i$ the mean field correction, the method of POD consists in choosing a complete orthonormal basis $V = \{\mathbf{v}_i\},\ i = 1, .., k;\ k > 0;\ v_i \in I\!R^n;\ V \in I\!R^{n\times k}$ such that the mean square error between $\mathbf{y}(t)$ and POD expansion $\mathbf{y}^{POD}(t) = \bar{\mathbf{y}} + V\tilde{\mathbf{y}}(t),\ \tilde{\mathbf{y}}(t) \in I\!R^k$ is minimized on average. Define $I(m) = \frac{\sum_{i=1}^{m}\lambda_i}{\sum_{i=1}^{n}\lambda_i}$ and k is chosen such that $k = \min\{I(m) : I(m) \geq \gamma\}$ where $0 \leq \gamma \leq 1$ is larger then 99% of the total kinetic energy captured by the reduced space $\text{span}\{\mathbf{v}_1, \mathbf{v}_2, ..., \mathbf{v}_k\}$.

By employing a Galerkin projection, the full model equations (3) is projected onto the space V spanned by the POD basis elements and the POD reduced order model is obtained

$$\frac{d\tilde{\mathbf{y}}(t)}{dt} = V^T\mathbf{F}\Big(\bar{\mathbf{y}} + V\tilde{\mathbf{y}}(t), t\Big), \quad \tilde{\mathbf{y}}(0) = V^T\Big(\mathbf{y}(0) - \bar{\mathbf{y}}\Big). \tag{4}$$

The efficiency of the POD-Galerkin technique is limited to linear or bilinear terms, since the projected nonlinear terms still depend on all the variables of the full model. To mitigate this inefficiency the *discrete empirical interpolation method* (DEIM) [6, 7, 8, 15] and the *empirical interpolation method* (EIM) [4, 13, 16] approximate the nonlinear terms via effective affine offline-online computational decompositions.

The projected nonlinearity in the system (4) is approximated by DEIM in the form that enables precomputation, so that evaluating the approximate nonlinear terms using DEIM does not require a prolongation of the reduced state variables back to the original high dimensional state approximation, as it is required for nonlinearity evaluation in the original POD approximation. Only a few entries of the original nonlinear term, corresponding to the specially selected interpolation indices from DEIM must be evaluated at each time step ([4, 6, 7, 11, 22]). We give formally the DEIM approximation in Definition 1, and the procedure for selecting DEIM indices is shown in Algorithm DEIM. Each DEIM index is selected to limit growth of a global error bound for nonlinear terms using a greedy technique ([7]).

Definition 1 Let $\{\mathbf{u}_\ell\}_{\ell=1}^m \subset I\!R^n$ be a linearly independent set computed from the snapshots of nonlinear term $\mathbf{F}$ in (3). The DEIM approximation of order m for $\mathbf{F}$ in the space spanned by $\{\mathbf{u}_\ell\}_{\ell=1}^m$ is given by

$$\mathbf{F} := \mathbf{U}(\mathbf{P}^T\mathbf{U})^{-1}\mathbf{P}^T\mathbf{F}, \tag{5}$$

where $\mathbf{P} = [\mathbf{e}_{\varrho_1}, \ldots, \mathbf{e}_{\varrho_m}] \in I\!R^{n\times m}$ with $\{\varrho_1, \ldots, \varrho_m\}$ being the output of Algorithm DEIM with the input basis $\{\mathbf{u}_i\}_{i=1}^m$.

Algorithm DEIM:
INPUT: $\{\mathbf{u}_\ell\}_{\ell=1}^m \subset I\!R^n$ linearly independent
OUTPUT: $\vec{\varrho} = [\varrho_1, \ldots, \varrho_m]^T \in I\!R^m$

1. $[|\rho|\ \varrho_1] = \max\{|\mathbf{u}_1|\}$
2. $\mathbf{U} = [\mathbf{u}_1],\ \mathbf{P} = [\mathbf{e}_{\varrho_1}],\ \vec{\varrho} = [\varrho_1]$
3. **for** $\ell = 2$ to m **do**
4. Solve $(\mathbf{P}^T\mathbf{U})\mathbf{c} = \mathbf{P}^T\mathbf{u}_\ell$ for $\mathbf{c}$
5. $\mathbf{r} = \mathbf{u}_\ell - \mathbf{U}\mathbf{c}$
6. $[|\rho|\ \varrho_\ell] = \max\{|\mathbf{r}|\}$
7. $\mathbf{U} \leftarrow [\mathbf{U}\ \mathbf{u}_\ell],\ \mathbf{P} \leftarrow [\mathbf{P}\ \mathbf{e}_{\varrho_\ell}],\ \vec{\varrho} \leftarrow \begin{bmatrix} \vec{\varrho} \\ \varrho_\ell \end{bmatrix}$
8. **end for**

In the Algorithm DEIM we denoted by "max" the built-in Matlab function *max* with the same significance. Thus, this function applied in step 6 by $[|\rho|\ \varrho_\ell] = \max\{|\mathbf{r}|\}$ leads to $|\rho| = |r_{\varrho_\ell}| = \max_{i=1,\ldots,n}\{|r_i|\}$, with the smallest index taken when the values along $|\mathbf{r}|$ contain more than one maximal element. Precisely, the index of the first one is returned. According to this algorithm, the DEIM procedure generates a set of indices inductively on the input basis in such a way that, at each iteration, the current selected index captures the maximum variation of the input basis vectors. The vector $\mathbf{r}$ can be viewed as the error between the input basis $\{\mathbf{u}_\ell\}_{\ell=1}^m$ and its approximation $\mathbf{Uc}$ from interpolating the basis $\{\mathbf{u}_\ell\}_{\ell=1}^{m-1}$ at the indices $\varrho_1, \ldots, \varrho_{m-1}$. The linear independence of the input basis $\{\mathbf{u}_\ell\}_{\ell=1}^m$ guarantees that, at each iteration, $\mathbf{r}$ is a nonzero vector and the output indices $\varrho_1, \ldots, \varrho_m$ are not repeating.

The POD and POD-DEIM reduced order models of system (2) were developed by using a Galerkin projection and the techniques presented in this section.

4 Numerical results

The system (2) was solved numerically using a finite difference discretization. Let $0 = x_0 < x_1 < \cdots < x_n < x_{n+1} = 1$ be equally spaced points on the x-axis for generating the grid points on the dimensionless domain $\Omega = [0, 1]$, and take time domain $[0, T] = [0, 1]$. The corresponding spatial finite difference discretized system of (2) becomes a system of nonlinear ODEs. The semi-implicit Euler scheme was used to solve the discretized system of full dimension and POD and POD-DEIM reduced order systems.

The parameters were set to the following values ([18]): $D_N = D_M =$ 8.e-8, $D_P = D_Q =$ 7.5e-7, $D_K =$ 1.25e-6, $\chi_P =$ 1.5e-5, $\chi_Q =$ 1.5e-5, $\rho_1 = 2.5$, $\rho_2 = 0.25$, $\rho_3 = 2.5$, $\gamma_1 = 0.8$, $\gamma_2 = 0.01$, $\gamma_3 = 1$, $s_1 = 0.8$, $s_2 = 0.2$, $s_3 = 0.8$, $c_1 = 0.3$, $c_2 = 0.004$, $c_3 = 0.2$, $\gamma_1 = 0.2$, $\gamma_2 = 0.1$ and $\gamma_3 = 0.01$. In our simulations we used the following initial conditions:

$$\begin{aligned}
N_0(x) &= x(1-x)[0.75e^{-100(x-0.5)^2} + 0.25e^{-100(x-0.15)^2}],\\
M_0(x) &= x(1-x)[0.15e^{-100(x-0.35)^2} + 0.65e^{-100(x-0.5)^2}],\\
P_0(x) &= x(1-x)[0.075e^{-100(x-0.25)^2} + 0.075e^{-125(x-0.75)^2}],\\
P_0(x) &= x(1-x)[0.075e^{-125(x-0.15)^2} + 0.095e^{-175(x-0.65)^2}],
\end{aligned}$$

and $K_0(x) = 0$. The number of spatial inner grid points on the x-axis – which defines the dimension of the full-order system – was successively

taken as 32, 64, 128, ..., 2048. For space configuration using 2048 points, the solution components of the problem (2) are depicted in Figs. 1,2. Tables 1–3 and Figs. 3–5 show a significant improvement in computational time of the POD-DEIM reduced system from both the POD reduced and the full-order system. Precisely, POD-DEIM reduces the computational time by a factor of $\mathcal{O}(10^2)$. The CPU time used in computing POD reduced system clearly reflects the dependency on the dimension of the original full-order system.

5 Conclusions

The model reduction technique combining POD with DEIM has been demonstrated to be efficient for capturing the spatio-temporal dynamics of a multi-species host-parasitoid system with substantial reduction in both dimension and computational time by a factor of $\mathcal{O}(10^2)$. The failure to decrease complexity with the standard POD technique was clearly demonstrated by the comparative computational times shown in Tables 1–4 and Figs 3–5. DEIM was shown to be very effective in overcoming the deficiencies of POD with respect to the nonlinearities in the model under study. In order to increase the efficiency of the POD-DEIM approximation, a possible extension is to incorporate the POD-DEIM approach with higher-order FD schemes to improve the overall accuracy, especially due to the spatio-temporal heterogeneity and chemotaxis driven instability.

We are also interested to compare the Discrete Empirical Interpolation Method with Gappy POD and Missing Point Estimation methods in the proper orthogonal decomposition framework applied to a higher order finite difference parasitoid model. The gappy POD procedure uses a POD basis to reconstruct missing, or "gappy" data and it was developed by [12]. The Missing Point Estimation method [2] relies on gappy POD technique and the reduced order model computes the Galerkin projections over a restricted subset of the spatial domain.

Acknowledgement. The first author acknowledges the support of the grant of the Romanian National Authority for Scientific Research, CNCS - UEFISCDI, project number PN-II-ID-PCE-2011-3-0563, contract no. 343/ 5.10.2011 "Models from medicine and biology: mathematical and numerical insights".

Table 1: CPU time of full-order system, POD and POD-DEIM reduced systems.

Internal Nodes n	CPU Time Full Dim	CPU Time POD	CPU Time POD–DEIM
32	5.407969e+00	5.317957e+00	1.715911e-01
64	5.254361e+00	5.347111e+00	1.680101e-01
128	5.607438e+00	5.710571e+00	1.696068e-01
256	6.847215e+00	6.614301e+00	1.809442e-01
512	8.610269e+00	7.600184e+00	2.016218e-01
1024	1.337721e+01	9.417793e+00	1.835292e-01
2048	2.653383e+01	1.312482e+01	1.812312e-01

Table 2: POD and POD-DEIM average relative errors for the components N and M – host species.

Internal Nodes n	$Error^{rel}$ POD – N	$Error^{rel}$ POD–DEIM – N	$Error^{rel}$ POD – M	$Error^{rel}$ POD–DEIM – M
32	3.482843e-14	3.516461e-14	1.645643e-13	1.657210e-13
64	1.388416e-14	1.414009e-14	9.331344e-14	9.348847e-14
128	1.653464e-14	1.661955e-14	7.420785e-14	7.175778e-14
256	4.718024e-15	4.669319e-15	1.590888e-14	1.634144e-14
512	2.736167e-14	2.732722e-14	1.716102e-14	2.124873e-14
1024	2.993938e-14	3.012212e-14	1.859783e-14	3.643836e-14
2048	9.590961e-15	1.042055e-14	4.956752e-14	1.216911e-13

Table 3: POD and POD-DEIM average relative errors for the components P and Q – parasitoid species.

Internal Nodes n	$Error^{rel}$ POD – P	$Error^{rel}$ POD–DEIM – P	$Error^{rel}$ POD – Q	$Error^{rel}$ POD–DEIM – Q
32	2.460205e-14	2.459944e-14	1.961488e-14	1.961738e-14
64	6.814060e-14	6.817415e-14	3.010484e-14	2.997920e-14
128	8.805397e-15	8.808601e-15	2.347853e-14	2.483260e-14
256	8.218387e-15	8.221235e-15	3.326519e-14	3.230054e-14
512	6.303037e-15	6.304210e-15	4.516320e-15	4.445458e-15
1024	1.758562e-14	1.720852e-14	3.067915e-15	3.980249e-15
2048	5.855724e-15	9.105957e-15	1.085525e-14	1.340351e-14

Table 4: POD and POD-DEIM average relative errors for the component K – chemoattractant.

Internal Nodes n	$Error^{rel}$ POD – K	$Error^{rel}$ POD–DEIM – K
32	5.987349e-14	6.004292e-14
64	3.937026e-14	3.981359e-14
128	3.118464e-14	3.054254e-14
256	1.440359e-14	1.604336e-14
512	3.286988e-14	3.330396e-14
1024	1.140597e-14	1.642880e-14
2048	2.154869e-14	4.431176e-14

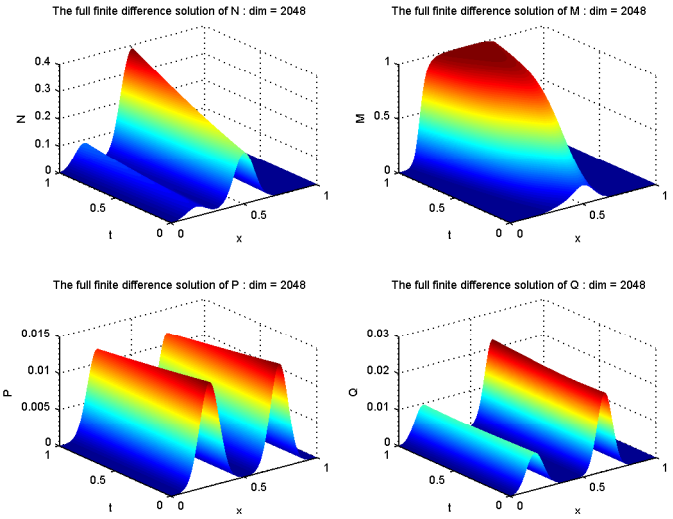

Figure 1: Solution plots (N, M, P, Q) of the model from the full-order system of dimension 2048.

References

[1] A.C. Antoulas. *Approximation of Large-Scale Dynamical Systems.* Advances in Design and Control. SIAM, Philadelphia, 2005.

[2] P. Astrid, S. Weiland, K. Willcox, T. Backx. Missing point estimation in models described by proper orthogonal decomposition. *IEEE Trans. Automat. Control.* 53(10):2237–2251, 2008.

[3] J.A. Atwell, B.B. King. Proper orthogonal decomposition for reduced

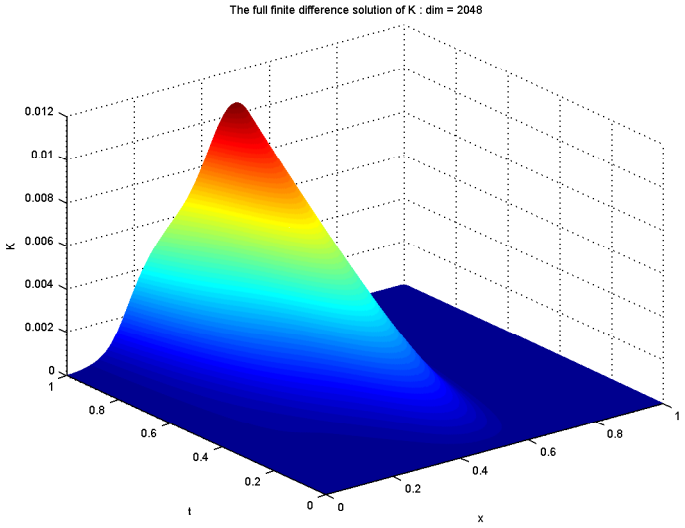

Figure 2: Solution plot K of the model from the full-order system of dimension 2048.

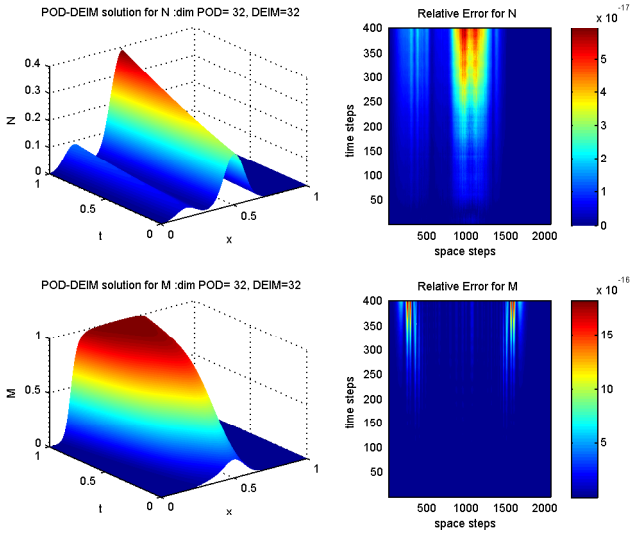

Figure 3: Solution plots (N, M) of the model from POD-DEIM reduced system (dimPOD=dimDEIM=32), with the corresponding average relative errors at the inner grid points ($n = 2048$).

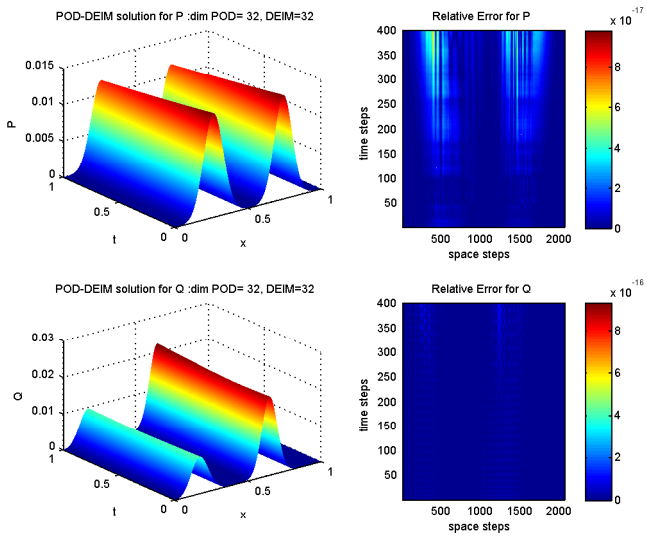

Figure 4: Solution plots (P, Q) of the model from POD-DEIM reduced system (dimPOD=dimDEIM=32), with the corresponding average relative errors at the inner grid points ($n = 2048$).

basis feedback controllers for parabolic equations. *Math. Comput. Modelling.* 33(1-3):1–19, 2001.

[4] M. Barrault, Y. Maday, N.C. Nguyen, A.T. Patera. An "empirical interpolation" method: application to efficient reduced-basis discretization of partial differential equations. *C.R. Math. Acad. Sci. Paris.* 339(9):667–672, 2004.

[5] G. Berkooz, P. Holmes, J. Lumley. The proper orthogonal decomposition in the analysis of turbulent flows. *Ann. Rev. Fluid Mech.* 25:777–786, 1993.

[6] S. Chaturantabut. Dimension Reduction for Unsteady Nonlinear Partial Differential Equations via Empirical Interpolation Methods. Technical Report TR09-38, CAAM, Rice University, 2008.

[7] S. Chaturantabut, D.C. Sorensen. Nonlinear model reduction via discrete empirical interpolation. *SIAM J. Sci. Comput.* 32(5):2737–2764, 2010.

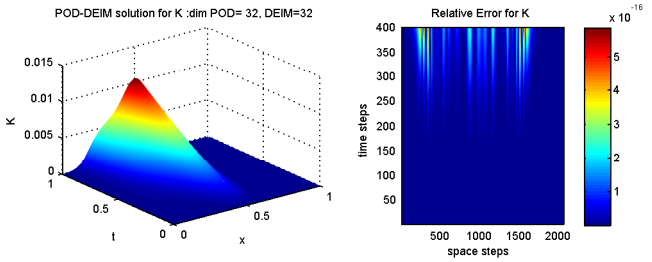

Figure 5: Solution plots K of the model from POD-DEIM reduced system (dimPOD=dimDEIM=32), with the corresponding average relative errors at the inner grid points ($n = 2048$).

[8] S. Chaturantabut, D.C. Sorensen. A state space error estimate for POD-DEIM nonlinear model reduction. *SIAM J. Numer. Anal.* 50(1):46–63, 2012.

[9] G. Dimitriu, N. Apreutesei. Comparative study with data assimilation experiments using proper orthogonal decomposition method. *Lecture Notes in Comput. Sci.* 4818:393–400, 2008.

[10] G. Dimitriu, N. Apreutesei, R. Ştefănescu. Numerical simulations with data assimilation using an adaptive POD procedure. *Lecture Notes in Comput. Sci.* 5910:165–172, 2010.

[11] G. Dimitriu, I.M. Navon, R. Ştefănescu. Application of POD-DEIM Approach for Dimension Reduction of a Diffusive Predator-Prey System with Allee Effect. *Lecture Notes in Comput. Sci.* 8353:373–381, 2014.

[12] R. Everson, L. Sirovich. Karhunen-Loève procedure for gappy data. *J. Opt. Soc. Am.* A 12:1657–1664, 1995.

[13] M.A. Grepl, Y. Maday, N.C. Nguyen, A.T. Patera. Efficient reduced-basis treatment nonaffine and nonlinear partial differential equations. *ESAIM Modélisation Mathématique et Analyse Numérique.* 41(3):575–605, 2007.

[14] K. Kunisch, S. Volkwein. Control of the Burgers' equation by a reduced order approach using proper orthogonal decomposition. *J. Optim. Theory Appl.* 102(2):345–371, 1999.

[15] O. Lass, S. Volkwein. POD Galerkin schemes for nonlinear elliptic-parabolic systems. *Konstanzer Schriften in Mathematik.* 301:1430–3558, 2012.

[16] Y. Maday, N.C. Nguyen, A.T. Patera, G.S.H. Pau. A General Multipurpose Interpolation Procedure: the Magic Points. *Commun. Pure Appl. Anal.* 8(1):383–404, 2009.

[17] I.G. Pearce, M.A.J. Chaplain, P.G. Schofield, A.R.A. Anderson, S.F. Hubbard. Modelling the spatio-temporal dynamics of multi-species host-parasitoid interactions: heterogeneous patterns and ecological implications. *J. Theor. Biol.* 241:876–886, 2006.

[18] I.G. Pearce, M.A.J. Chaplain, P.G. Schofield, A.R.A. Anderson, S.F. Hubbard. Chemotaxis-induced spation-temporal heterogeneity in multi-species host-parasitoid systems. *J. Math. Biol.* 55:365–388.

[19] L. Sirovich. Turbulence and the dynamics of coherent structures. I. Coherent structures. *Quart. Appl. Math.* 45(3):561–571, 1987.

[20] L. Sirovich. Turbulence and the dynamics of coherent structures. II. Symmetries and transformations. *Quart. Appl. Math.* 45(3):573–582, 1987.

[21] L. Sirovich. Turbulence and the dynamics of coherent structures. III. Dynamics and scaling. *Quart. Appl. Math.* 45(3):583–590, 1987.

[22] R. Ştefănescu, I.M. Navon. POD/DEIM nonlinear model order reduction of an ADI implicit shallow water equations model. *J. Comput. Phys.* 237:95–114, 2013.